

CHAPTER II

BACKGROUND

2.1 MR PHYSICS

2.1.1 Magnetized Nuclear Spin Systems

The NMR phenomenon is based on the chemistry and biophysical properties of subatomic levels of the nuclei that have a basic physical property, called *spin*. The unpaired nuclear particles that have odd atomic weights and/or odd atomic numbers, such as the nucleus of the hydrogen atom (which has one proton), possess an angular momentum \vec{J} , have *spin* or *spin angular momentum* (which is from spin + mass). Another property is magnetic moment which is the magnetic field around the spinning charges. The two important reasons generating the magnetic field of nuclei are: 1) electrical charges, and 2) nonzero spin angular momentum. The spinning charge creates a magnetic field around it, which is analogous to a tiny bar magnet, as shown in figure 2.1, which is represented by a vector quantity $\vec{\mu}$ that is called the nuclear *magnetic dipole moment* or *magnetic moment* (which is from spin + charge).

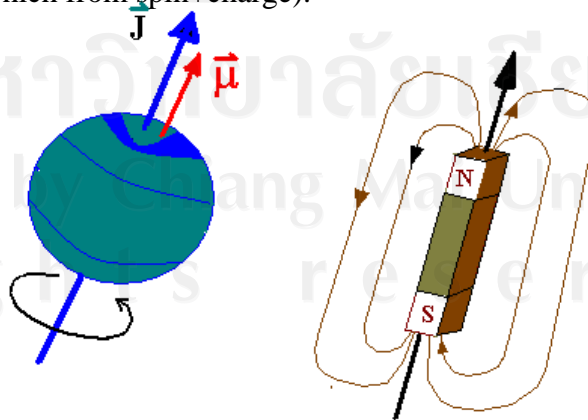


Figure 2.1 Nonzero spin and magnetic moment are regarded as tiny bar magnet

The relationship of spin angular momentum and magnetic moment is

$$\vec{\mu} = \gamma \vec{J} \quad (2.1)$$

Where γ is a physical constant known as the *gyromagnetic ratio* or *magnetogyric ratio*. The magnitude of μ is

$$|\mu| = \gamma \hbar \sqrt{I(I+1)} \quad (2.2)$$

Where I is the *nuclear spin quantum number* that takes integer or half-integer or zero values such that $I = 0, 1/2, 1, 3/2, 2 \dots$ and \hbar is Planck's constant ($6.6 \times 10^{-34} \text{ jule.sec}$) over the constant 2π . The values of I following the three simple rules[11]:

- 1) Nuclei with an *odd mass number* have **half-integral spin**.
- 2) Nuclei with an *even mass number and an even charge number* (depend on difference of proton and neutrons) have **zero spin**.
- 3) Nuclei with an *even mass number but an odd charge number* have **integral spin**.

The magnitude of magnetic moment is certain under any condition (with or without an external magnetic field), but its direction is completely random in without external magnetic field due to thermal random motion. When placed magnetic moment of spin

system in a strong external magnetic field of strength B_0 that applied in the z-direction of

laboratory frame or $\vec{B} = B_0 \vec{k}$. By quantum theory, the magnetic moment vector in

Z-component of the $\vec{\mu}$ is

$$\mu_z = \gamma m_I \hbar \quad (2.3)$$

Where m_l is called the *magnetic quantum number*, that takes the following set of $(2I+1)$ values: $m_l = -I, -I+1, \dots, I$ that corresponds to possible orientations for magnetic moment ($\vec{\mu}$) with respect to the direction of the external field. The angle between $\vec{\mu}$ and B_0 can be calculated by

$$\cos \theta = \frac{\mu_z}{\mu} = \frac{m_l}{\sqrt{I(I+1)}} \quad (2.4)$$

For a half-integral spin (such as hydrogen atom) system can be calculated based on Eqs.(2.4) is

$$\theta = \cos^{-1} \left(\frac{1/2 \text{ or } -1/2}{\sqrt{1/2(1/2+1)}} \right) = \pm \left(0.9553 \times \frac{180}{\pi} \right) = \pm 54.74^\circ \quad (2.5)$$

as shown in figure 2.2

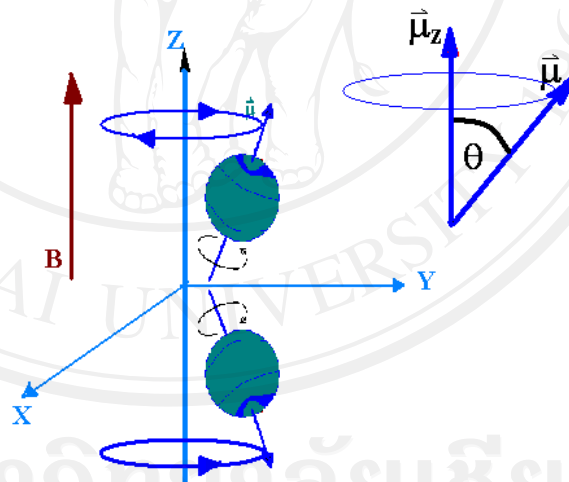


Figure 2.2 Precession of two opposing directions of nuclear spin about an external magnetic field

The transverse component or $\vec{\mu}_{xy}$ that remains random distributed over $[0, 2\pi)$ and its magnitude is

$$|\vec{\mu}_{xy}| = \sqrt{\mu^2 - \mu_z^2} = \gamma \hbar \sqrt{I(I+1) - m_l^2} = \frac{\gamma \hbar}{\sqrt{2}} \quad (2.6)$$

The classical mechanics:

By assuming that each $\vec{\mu}$ without mutual interactions, the torque or turning force tries to align $\vec{\mu}$ with \vec{B}_0 but nucleus has an angular momentum so it does not simply to align $\vec{\mu}$ with \vec{B}_0 . For the conservation of angular momentum, torque is equal to the rate of change of its angular momentum, hence

$$\frac{d\vec{J}}{dt} = \frac{1}{\gamma} \frac{d\vec{\mu}}{dt} = \vec{\mu} \times B_0 \vec{k} \quad (2.7)$$

then

$$\frac{d\vec{\mu}}{dt} = \vec{\mu} \times \gamma B_0 \vec{k} \quad (2.8)$$

Eqs.(2.8) can be written as

$$\frac{d\vec{\mu}}{dt} = \gamma \begin{vmatrix} \vec{i} & \vec{j} & \vec{k} \\ \mu_x & \mu_y & \mu_z \\ 0 & 0 & B_0 \end{vmatrix} = \gamma(B_0 \mu_y \vec{i} - B_0 \mu_x \vec{j}) \quad (2.9)$$

then,

$$\begin{aligned} \frac{d\mu_x}{dt} &= \omega_0 \mu_y \\ \frac{d\mu_y}{dt} &= -\omega_0 \mu_x \\ \frac{d\mu_z}{dt} &= 0 \end{aligned} \quad (2.10)$$

Decoupling after 2nd derivatives with respect to time, then

$$\frac{d^2 \mu_x}{dt^2} = \frac{d\left(\frac{d\mu_x}{dt}\right)}{dt} = \frac{d(\omega_0 \mu_y)}{dt} = \omega_0 \frac{d\mu_y}{dt} = -\omega_0^2 \mu_x \quad (2.11)$$

Likewise, y direction becomes

$$\frac{d^2 \mu_y}{dt^2} = -\omega_0^2 \mu_y \quad (2.12)$$

These decoupled 2nd order differential equations and the solutions, for the initial conditions to $\mu_x(0)$, $\mu_y(0)$ and $\mu_z(0)$ are:

Solved

$$-\omega_0^2 \mu_y = \frac{d^2(\mu_y)}{dt^2} = \mu_y''$$

$$-\omega_0^2 \mu_x = \frac{d^2(\mu_x)}{dt^2} = \mu_x''$$

For harmonic differential equation we can use guess solution, that is

$$\text{if } \mu = e^{mt} \therefore \mu' = me^{mt}, \mu'' = m^2 e^{mt}$$

$$m^2 + \omega_0^2 = 0$$

$$m = i\omega_0$$

that is the complex root, the solution is in the form of

$$e^{\text{real}(t)} A \cos(\text{imag}(t)) + B \sin(\text{imag}(t));$$

then,

$$\mu_x(t) = e^0 (A \cos(\omega_0 t) + B \sin(\omega_0 t))$$

$$\mu_y(t) = \left(\frac{d\mu_x}{dt} \right) / \omega_0 = -A \sin(\omega_0 t) + B \cos(\omega_0 t)$$

at $t=0$, the above equations become

$$\mu_x(0) = A, \mu_y(0) = B;$$

then the solution is

$$\begin{cases} \mu_x(t) = \mu_x(0) \cos(\omega_0 t) + \mu_y(0) \sin(\omega_0 t) \\ \mu_y(t) = -\mu_x(0) \sin(\omega_0 t) + \mu_y(0) \cos(\omega_0 t) \\ \mu_z(t) = \mu_z(0) \end{cases} \quad (2.13)$$

The complex notation of isolated spins is

$$\begin{cases} \mu_{xy}(t) = \mu_{xy}(0) e^{-i\omega_0 t} \\ \mu_z(t) = \mu_z(0) \end{cases} \quad (2.14)$$

From equation (2.14), on the laboratory frame, we can see $\bar{\mu}$ when it is placed in an external magnetic field, which precession about the B_0 field: called *Nuclear precession*; and the transverse component changes to a given time, however the vertical or longitudinal component does not change, as illustrated in figure 2.3

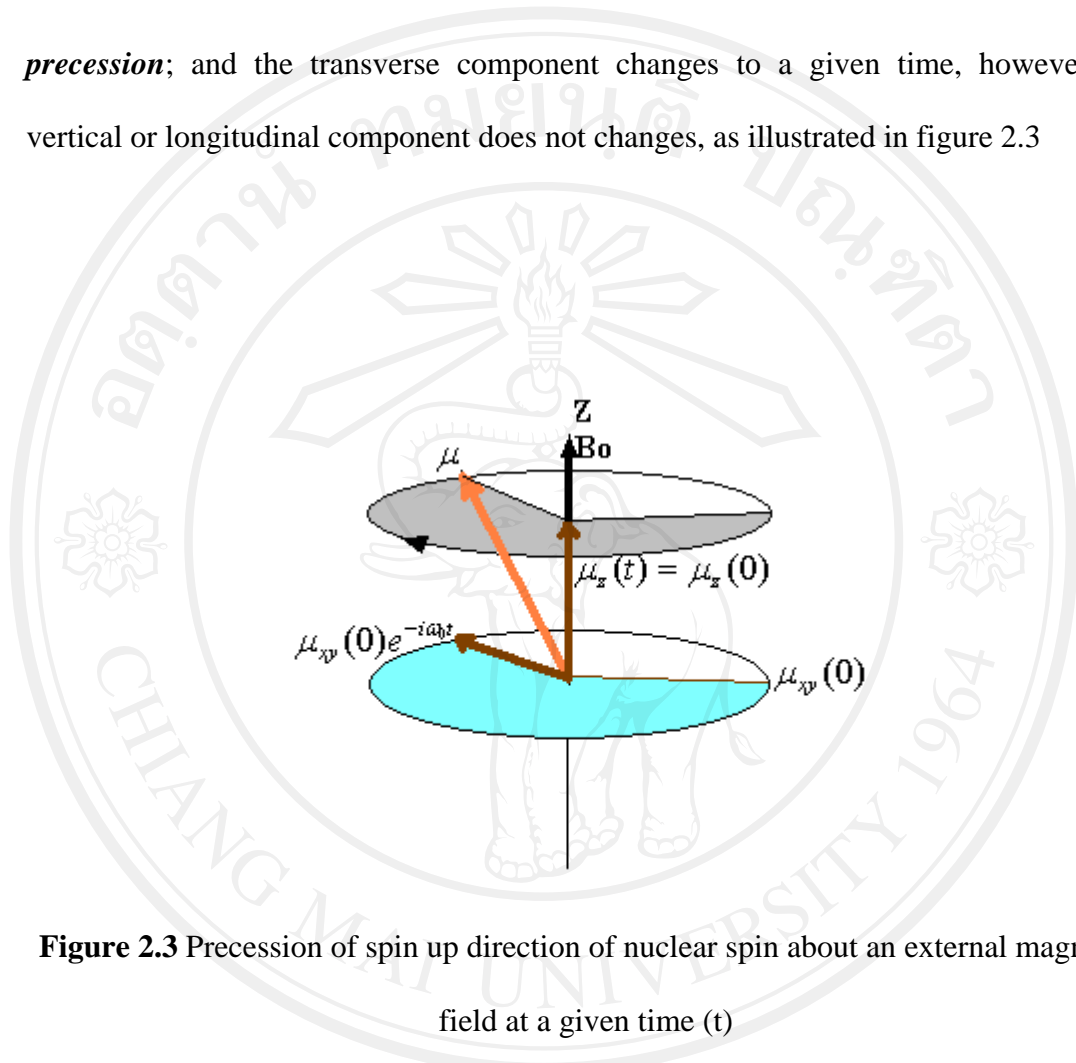


Figure 2.3 Precession of spin up direction of nuclear spin about an external magnetic field at a given time (t)

For the transverse vector that has changes in a given time was opposite direction of the direction of spin, which is $-\omega_0$ or the left hand rule. The rotations in 3D space are specified by rotation about z-axis and rotation angle $(\omega_0 t)$ that for nuclear precession and right hand rule for spin cause of positive charge and the modulus of frequency given by

$$\omega = \gamma B_0 \text{ rad/sec}$$

and the frequency is
$$f = \frac{\gamma}{2\pi} B_0 \quad \text{Hz.} \quad (2.15)$$

2.1.2 Bulk Magnetization

In MRI, it is convenient to consider the local magnetic dipole moment per unit volume, or the magnetization is

$$M = \sum_{i=1}^N \mu_i \quad (2.16)$$

Where μ_i is the magnetic moment of the i -th nuclear spins and N is the total number of spins. With an assumption of homogeneous sample and uniform field, when external magnetic field is applied, there is a torque to M by B_0 resulting in nuclear precession at the Larmor frequency as in Eqs.2.8 which is

$$\frac{d\vec{M}}{dt} = \vec{M} \times \gamma B_0 \vec{k} \quad (2.17)$$

According to the Eqs2.9-2.14, when magnetization vector precesses (nutate) about z axis, the direction of applied field at an angular frequency of ω_0 in a matrix form is

$$\begin{pmatrix} \frac{dM_x}{dt} \\ \frac{dM_y}{dt} \\ \frac{dM_z}{dt} \end{pmatrix} = \gamma \begin{pmatrix} 0 & B_0 & 0 \\ -B_0 & 0 & 0 \\ 0 & 0 & 0 \end{pmatrix} \begin{pmatrix} M_x \\ M_y \\ M_z \end{pmatrix} \quad (2.18)$$

The cross-coupling of the M_x and M_y components leads to a solution of [12]

$$M(t) = \begin{pmatrix} M_x(t) \\ M_y(t) \\ M_z(t) \end{pmatrix} = \begin{pmatrix} \cos(\omega_0 t) & \sin(\omega_0 t) & 0 \\ -\sin(\omega_0 t) & \cos(\omega_0 t) & 0 \\ 0 & 0 & 1 \end{pmatrix} M_z^0 \quad (2.19)$$

, where M_z^0 = Net magnetizations at $t=0$ and $\omega_0 = \gamma B_0$ = Larmor Frequency

2.1.3 The Bloch Equation and Relaxation Time

Eqs (2.14) has been applied in magnetic dipole moment even in microscopic viewpoint. If the term containing T_1 and T_2 are included, the Bloch equation written in general form becomes

$$\frac{d\vec{M}}{dt} = \gamma\vec{M} \times \vec{B} - \frac{M_x\vec{i} + M_y\vec{j}}{T_2} - \frac{(M_z - M_z^0)\vec{k}}{T_1} \quad (2.20)$$

Where M_z^0 is the thermal equilibrium value of magnetization in the presence of only B_0 .

T_1 and T_2 are time constants of the relaxation process of a spin system after it has been disturbed from thermal equilibrium. In the rotating frame, the general Bloch equation can be expressed as

$$\frac{\partial\vec{M}_{rot}}{\partial t} = \gamma\vec{M}_{rot} \times \vec{B}_{eff} - \frac{M_x\vec{i}' + M_y\vec{j}'}{T_2} - \frac{(M_z' - M_z^0)\vec{k}'}{T_1} \quad (2.21)$$

Where $\vec{B}_{eff} = \vec{B}_{rot} + \frac{\vec{\omega}}{\gamma}$, if $\vec{B}_{rot} = B_0\vec{k}$ the magnetization \vec{M}_{rot} appears to be a stationary in the rotating frame.

The Matrix from of Bloch equation is

$$\begin{pmatrix} \frac{dM_x}{dt} \\ \frac{dM_y}{dt} \\ \frac{dM_z}{dt} \end{pmatrix} = \begin{pmatrix} -\frac{1}{T_2} & \gamma B_0 & 0 \\ -\gamma B_0 & -\frac{1}{T_2} & 0 \\ 0 & 0 & -\frac{1}{T_1} \end{pmatrix} \begin{pmatrix} M_x \\ M_y \\ M_z \end{pmatrix} + \begin{pmatrix} 0 \\ 0 \\ \frac{M_0}{T_1} \end{pmatrix} \quad (2.22)$$

hence, the solution is

$$M_{xyz}(t) = \begin{pmatrix} e^{-t/T_2} & 0 & 0 \\ 0 & e^{-t/T_2} & 0 \\ 0 & 0 & e^{-t/T_1} \end{pmatrix} \begin{pmatrix} \cos(\omega_0 t) & \sin(\omega_0 t) & 0 \\ -\sin(\omega_0 t) & \cos(\omega_0 t) & 0 \\ 0 & 0 & 1 \end{pmatrix} M_z^0 + \begin{pmatrix} 0 \\ 0 \\ M_z^0(1 - e^{-t/T_1}) \end{pmatrix} \quad (2.23)$$

The exponential term represents the decay of precessing magnetization in the transverse (x,y) plane with a time constant T_2 . Simultaneously, the longitudinal magnetization returns to equilibrium position along the longitudinal axis (z) at a rate determined by a time constant T_1 .

The transverse magnetization, M_{xy} can be decomposed into 2 components (Real and imaginary parts) as in Eqs. 2.24

$$M_{xy} = M_x + iM_y \quad (2.24)$$

The Bloch equation for this case is now written as

$$\frac{dM_{xy}}{dt} = \frac{dM_x}{dt} + i \frac{dM_y}{dt} = -\left(\frac{1}{T_2} + i\omega_0\right) M_{xy} \quad (2.25)$$

and

$$\frac{dM_z}{dt} = -\frac{(M_z - M_0)}{T_1} \quad (2.26)$$

this is the first-order differential equation with a compact solution is

$$M_{xy}(t) = M_{xy}(0) e^{-t/T_2} e^{-i\omega_0 t} \quad (2.27)$$

representing decay of a complex exponential of frequency ω_0 . The original component' values related to M_{xy} at a given time are:

$$\text{Re}\{M_{xy}(t)\} = M_x, \quad \text{Im}\{M_{xy}(t)\} = M_y \quad (2.28)$$

2.2 THE RADIOFREQUENCY EXCITATION

2.2.1 Radiofrequency Magnetic Field

After the external magnetic field \vec{B}_0 is applied, the bulk magnetization M will align to the same direction of \vec{B}_0 . There is no transverse magnetization in this equilibrium state because the phases of individual magnetic moments in this bulk magnetization are distributed random and cancel each other. The excitation process is the way to establish *the phase coherences of these magnetic moments* so that a transverse magnetization is generated. In order to achieve the coherences of phase, an external force must be applied to the spin system. This external force provides an oscillating magnetic field or B_1 field which is perpendicular to the main magnetic field and rotates at the same angular frequency as the Larmor frequency to facilitate energy exchange. Reiteratively, RF magnetic pulse B_1 tuned to the resonance frequency of the spins is applied in the transverse plane to excite these spins out of equilibrium.

The term B_1 pulses or *RF pulse* is synonym of the B_1 field generation, so called because the frequency is normally between 1MHz and 500 MHz, corresponding to the radio waves.

In fact, many RF pulses are named based on the characteristics of this envelope function. For example; the widely used Rectangular function and Sinc pulse see figure

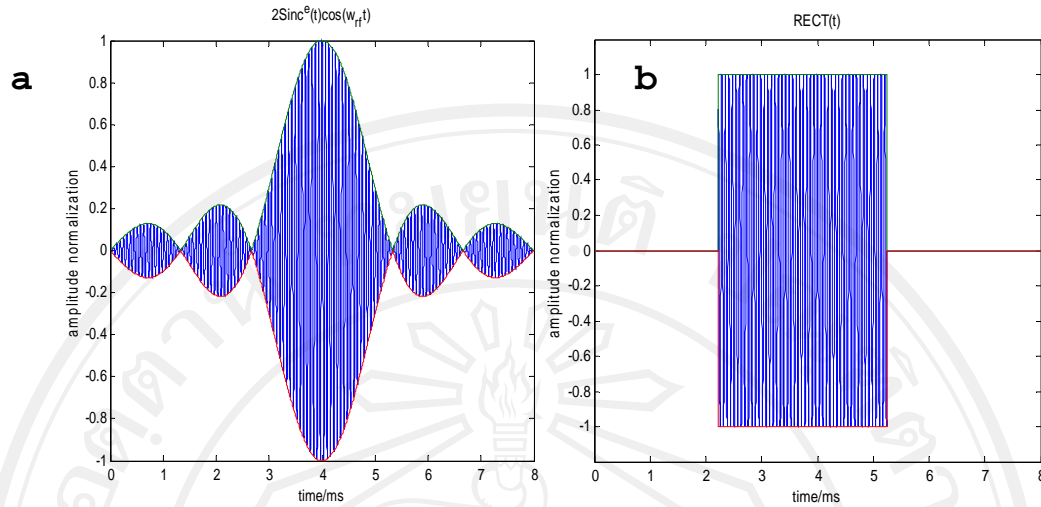


Figure 2.4(a) the amplitude modulated RF in sinc pulse (shapes) and **(b)** rectangular pulse (turn on and off)

Energy imparted from B_1 generates a torque to rotate the magnetization vectors as a prescribed angle depending on the strength of B_1 and its durations. The strength of B_1 is typically small amount fraction of a Gauss (10^{-4} Tesla); which is weakest field using in MRI (typical about $1/4.257$ Gauss)[13], and duration is usually in a few milliseconds.

A typical RF pulse can be described by an *amplitude modulated* sinusoidal function:

$$B_1(t) = 2B_1^e(t) \cos(\omega_{rf}t + \varphi) \quad (2.29)$$

where $B_1^e(t)$ is an envelope function that modulates the amplitude, ω_{rf} is the carrier frequency, and φ is the initial phase angle. If the φ is constant, it has no effect on excitation. It can be assumed as zero[11]. The complex notation can be decomposed into two rotating components:

$$B_1(t) = B_1^e(t)e^{i\omega_{rf}t} + B_1^e(t)e^{-i\omega_{rf}t} \quad (2.30)$$

The one rotating counterclockwise is called $B_1^-(t)$ has negligible effect on the magnetized spin system compared to the clockwise component which is called $B_1^+(t)$, and then the effective $B_1(t)$ field is $B_1^e e^{-i\omega_{rf}t}$ which can be written in matrix form as:

$$B_1(t) = \begin{bmatrix} B_{1x} \\ B_{1y} \end{bmatrix} = \begin{bmatrix} B_1^e \cos(\omega_{rf}t) \\ -B_1^e \sin(\omega_{rf}t) \end{bmatrix} \quad (2.31)$$

When B_1 is turn on, the magnetic field will be,

$$B = B_1(t)[\cos \omega_{rf}t - \sin \omega_{rf}t] \begin{bmatrix} i \\ j \end{bmatrix} + B_0 k \quad (2.32)$$

From Eqs.2.17 the magnetization is

$$\frac{d\vec{M}}{dt} = \vec{M} \times \gamma B \vec{k} = \vec{M} \times \gamma \{B_1(t)[\cos \omega_{rf}t \vec{i} - \sin \omega_{rf}t \vec{j}] + B_0 \vec{k}\} \quad (2.33)$$

the Eqs.2.24 in a matrix form is

$$\begin{pmatrix} \frac{dM_x}{dt} \\ \frac{dM_y}{dt} \\ \frac{dM_z}{dt} \end{pmatrix} = \begin{pmatrix} 0 & \gamma B_0 & -\gamma B_1(t) \sin \omega t \\ -\gamma B_0 & 0 & \gamma B_1(t) \cos \omega t \\ \gamma B_1(t) \sin \omega t & -\gamma B_1(t) \cos \omega t & 0 \end{pmatrix} \begin{pmatrix} M_x \\ M_y \\ M_z \end{pmatrix} \quad (2.34)$$

2.2.2 Rotating Frame

It is easier to consider the time dependence of magnetization in the rotating frame about z-axis which is the Larmor frequency in clockwise direction of the B_1 excitation field. In the rotating frame with the Larmor frequency, the precession of the spins is observed as stationary. Mathematically, the rotating frame can be express by a rotational matrix

$$R_{z(\omega_0 t)} = \begin{bmatrix} \cos(\omega_0 t) & -\sin(\omega_0 t) & 0 \\ \sin(\omega_0 t) & \cos(\omega_0 t) & 0 \\ 0 & 0 & 1 \end{bmatrix} \quad (2.35)$$

Rotating magnetization and B_1 are defined as

$$M_{rot} = \begin{pmatrix} M_{x'} \\ M_{y'} \\ M_{z'} \end{pmatrix}, B_{1rot} = \begin{pmatrix} B_{x'} \\ B_{y'} \\ B_{z'} \end{pmatrix} \quad (2.36)$$

The RF field B_1 is only applied in the transverse plane at the Larmor frequency. In the rotating frame, the B_1 field generally applies along a fixed x' axis and can be written in 2D matrix form as:

$$B_{1,rot} = R_{2d(\omega_0 t)} B_1 = \begin{bmatrix} \cos(\omega_0 t) & -\sin(\omega_0 t) \\ \sin(\omega_0 t) & \cos(\omega_0 t) \end{bmatrix} \begin{bmatrix} B_1^e \cos \omega_{rf} t \\ -B_1^e \sin(\omega_{rf} t) \end{bmatrix} = \begin{bmatrix} B_1^e \cos(0) \\ 0 \end{bmatrix} = [B_1^e i'] \quad (2.37)$$

The effective magnetic field B_{eff} becomes

$$B_{eff} = (B_0 - \frac{\omega_{rf}}{\gamma})k' + B_1^e i' \quad (2.38)$$

At the **on-resonance excitation condition** $\omega_{rf} = \omega_0$ then

$$B_{eff} = B_1^e i' \quad (2.39)$$

The only magnetic field observed in the rotating frame is B_1^e applied along the x prime axis. Practically, the high frequency part observed as a vector in the rotating frame is demodulated and the RF oscillation is transformed to the time-dependent envelope $B_1^e(t)$. The magnetization M will be tipped away from the z prime-axis to the y-prime axis. This is the reason of smaller B_1 field can tip the magnetization away from the direction of the much stronger main magnetic field. The angular frequency of this rotation resulted by the RF pulse will be;

$$\omega_1 = \gamma B_1^e \quad (2.40)$$

For the soft or tailored RF pulse, the flip angle is the time integral of the angular frequency over the pulse duration T ;

$$\alpha = \int_0^T \omega_1(t) dt = \gamma \int_0^T B_1^e(t) dt \quad (2.41)$$

Ignoring the relaxation effects of Bloch equation, it becomes

$$\frac{dM_{x'y'}}{dt} = -\gamma B_1^e(t) \times M_{x'y'} \quad (2.42)$$

The solution of this equation will be:

Solved: By the same way of find the solution Eqs.2.13

$$d\vec{M}_{rot} / dt = \begin{bmatrix} 0 & 0 & 0 \\ 0 & 0 & \gamma B_1 \\ 0 & -\gamma B_1 & 0 \end{bmatrix} \begin{bmatrix} M_{x'} \\ M_{y'} \\ M_{z'} \end{bmatrix}$$

$$dM_{x'} / dt = 0$$

$$dM_{y'} / dt = \gamma B_1^e(t) M_{z'}$$

$$dM_{z'} / dt = -\gamma B_1^e(t) M_{y'}$$

Decouples and use guess solution, $= i\omega_1$

that is the complex root, the solution is in the form of

$$e^{real(t)} A \cos(imag(t)) + B \sin(imag(t));$$

then,
$$M_{y'}(t) = e^0 (A \cos(\omega_1 t) + B \sin(\omega_1 t))$$

$$M_{z'}(t) = \left(\frac{dM_{y'}}{dt} \right) / \omega_1 = -A \sin(\omega_1 t) + B \cos(\omega_1 t)$$

at t=0, $M_{z'}(0) = M_z^0$ that is only B = $M_z(0)$;

then the solution is,

$$\begin{bmatrix} M_{x'}(t) \\ M_{y'}(t) \\ M_{z'}(t) \end{bmatrix} = \begin{bmatrix} 0 \\ M_z^0 \sin\left(\int_0^t \gamma B_1^e(t) dt\right) \\ M_z^0 \cos\left(\int_0^t \gamma B_1^e(t) dt\right) \end{bmatrix} = \begin{bmatrix} 0 \\ M_z^0 \sin(\alpha) \\ M_z^0 \cos(\alpha) \end{bmatrix} \quad (2.43)$$

, where α is the flip angle.

Apparently the bulk magnetization vector precesses about the x' -axis with angular velocity as shown on figure 2.5

$$\vec{\omega}_1 = -\gamma \vec{B}_1 \quad (2.44)$$

The precession of M about the B_1 field is called *forced precession* [11].

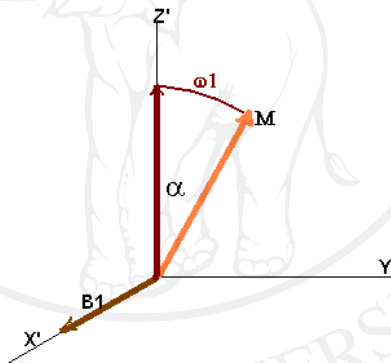


Figure 2.5 the Bulk magnetization vector in the presence of a rotating RF field in the RF rotating frame

From equation 2.41, if B_1 is turned on for a period of t_p , the tip (flip or rotation) angle θ in radians is

$$\theta = \int_0^{t_p} \gamma B_1(t) dt \quad \text{for general time-varying } B_1(t) \quad (2.45)$$

$$\theta = \gamma B_1 t_p \quad \text{for constant } B_1 \text{ (or hard pulse)} \quad (2.46)$$

2.2.3 Off-resonance condition:

There is no perfectly uniform B_0 within a given volume. This may be caused by hardware imperfections, chemical shifts, effect of the RF pulse, subject susceptibility

induced field variations and eddy current. Therefore, the main field can be considered as a space variant function. The difference of local main field to the RF tuning Larmor frequency is called the off-resonance, $\Delta\omega(r)$

$$\Delta\omega(r) = \omega(r) - \omega_0 \quad (2.47)$$

In the presence of off-resonance condition ($\omega_0 \neq \omega_{rf}$), the effective magnetic field B_{eff} will have an additional term along the z axis,

$$B_{eff} = \left(\frac{\omega(r)}{\gamma} - \frac{\omega_{rf}}{\gamma} \right) k' + B_1 i' = \frac{\Delta\omega}{\gamma} k' + B_1 i' \quad (2.48)$$

The Bloch equation in the rotating frame with the typical B_1 pointing along the x' axis and residual component $\Delta\omega/\gamma$ pointing along the z' -axis ignoring relaxation effects becomes

$$\frac{\partial \vec{M}_{rot}}{\partial t} = \begin{bmatrix} 0 & \Delta\omega & 0 \\ -\Delta\omega & 0 & \gamma B_1(t) \\ 0 & -\gamma B_1(t) & 0 \end{bmatrix} \begin{bmatrix} M_{x'} \\ M_{y'} \\ M_{z'} \end{bmatrix} \quad (2.49)$$

In general, there is no close-form solution for this equation. For a constant RF field or hard pulse, the solution of Bloch equation indeed exists, which is given by

$$\begin{aligned} M_{x'} &= M_Z^0 \sin \theta \cos \theta (1 - \cos \alpha) \\ M_{y'} &= M_Z^0 \sin \theta \sin \alpha \\ M_{z'} &= M_Z^0 (\cos^2 \theta + \sin^2 \theta \cos \alpha) \end{aligned} \quad \begin{aligned} & ; \alpha = T \sqrt{\Delta\omega^2 + \omega_1^2} \\ & ; \theta = \tan^{-1} \left(\frac{\omega_1}{\Delta\omega} \right) \end{aligned} \quad (2.50)$$

Where α is the tip angle about the axis of $B_{1,eff}$, then the transverse magnetization after excitation is not along the y' axis as in the case of on-resonance excitation but has a phase shift from y' axis. This phase shift can be problematic for some MRI applications. In addition, the magnitude of the transverse magnetization is given by

$$M_{xy'} = M_Z^0 \sin \theta \sqrt{\sin^2 \alpha + (1 - \cos \alpha)^2 \cos^2 \theta} \quad (2.51)$$

That decreases as the frequency offset increases (or T_2')

2.3 DATA ACQUISITION

2.3.1 Signal detection and reciprocity law

According to the time-varying magnetic fields and Faraday's Law, if a source is producing a magnetic field, then we can measure how much flux it will generate through a coil by measuring the induced voltage in a coil placed perpendicular to the direction of this magnetic field. The induced voltage or (electromotive forces, emf) is given by

$$V(t) = - \frac{\partial \Phi(t)}{\partial t} \quad (2.51)$$

Where Φ is the magnetic flux. In MRI, the measured voltages or signals from the coil determine the magnetic fields (in our case, spin distribution). According to the *principle of reciprocity*, if there are two identical coils, A and B, if coil A can produce flux through coil B, then coil B can also produce an identical amount of flux through coil A [14] and the flux, Φ is defined as

$$\Phi(t) = \int |B| \cdot \vec{n} \cdot da \quad (2.52)$$

Where B is the magnetic field perpendicular to the coil, and da is the surface area of the coil. In MRI, when the same RF coil is used for excitation and reception, the flux detected by the receiving coil can be determined through the principle of reciprocity

[14] as:

$$\Phi(t) = \int \vec{B}_r(r) \cdot M(r,t) dr \quad (2.53)$$

Substituting this into equation 2.50

$$V(t) = -\frac{\partial}{\partial t} \int \bar{B}_r(r) \cdot M(r, t) dr \quad (2.54)$$

Where \bar{B}_r is the laboratory frame magnetic field at location r per unit of direct current flowing in the receiver coil and M is the magnetization that produces the magnetic flux through the coil. Since the z component of the magnetization, M_z is a slowly varying function compared to the free precession of the M_x and M_y component, the M_z component can be ignored. That is why all people *often refer the MR signal as the transverse magnetization M_{xy}* . Therefore, the MR signals after the demodulation of the high frequency term, the signal equation in rotating frame [11].

$$s(t) = \omega_0 e^{i\pi/2} \int \bar{B}_{xy}^*(r) \cdot M_{xy}(r, 0) e^{-t/T_2(r)} \cdot e^{-i\Delta\omega(r)t} dr \quad (2.55)$$

Where B_{xy}^* is the complex conjugate of the transverse received magnetic field B_{xy} , or the “coil sensitivity”. The dependence of signal on the ‘transmit coil sensitivity’ is implicitly included in the magnetization M . Ignoring the T_2^* effect, the signal amplitude is proportional to the Larmor frequency, the coil sensitivity, the transverse magnetization, and the sample volume.

$$|S| \propto \omega_0 M_{xy} B_{xy}^* V_s \quad (2.56)$$

The Larmor frequency and the transverse magnetization are linearly related to the main magnetic field. That is why the high field MRI has the advantage on the image SNR.

2.3.2 Free Induction Decay (FID)

The time signal from a nuclear spin system is collected right after a single RF is applied. No gradient fields are involved here. The signal is call *Free Induction Decay (FID)*. “Free” refers to the signal generated by the free precession of the bulk

magnetization vector about the main magnetic field. “Induction ” indicates that the signal is produced base on electromagnetic induction[11]. “Decay” reflects the characteristic decrease with time of signal amplitude that loss of phase between spins and loss of energy from spins to surroundings. Mathematically, if the field inhomogeneity has Lorentzian distribution, the FID signal becomes

$$S(t) = Ae^{-\gamma\Delta B_0 t} e^{-t/T_2} e^{-i\omega_0 t} = Ae^{-t/T_2^*} e^{-i\omega_0 t} \quad (2.57)$$

Where

$$\frac{1}{T_2^*} = \frac{1}{T_2} + \gamma\Delta B_0 \quad (2.58)$$

Eqs.2.58 is valid for Lorentzian spectral density function, the envelope of FID signal will be exponential function, and T_2^* should be interpreted as the effective time constant of an approximating exponential, and A, magnitude of the signal from Eqs.2.57, is dependent on a number of parameter such as flip angle, the number of spins in sample and the magnetic field strength [10]. FID time signal depends on field inhomogeneity or T_2^* decay

2.3.4 Frequency encoding

After an excitation, the FID signal is localized by applying a gradient on one direction that is placed in an assuming homogeneous B_0 field, the Larmor frequency (precessions) will be linearly changed depending on each position, and the precession at position (x) is

$$\omega(x) = \gamma(B_0 + G_x x) \quad (2.59)$$

Consequently, the FID signal generated locally from spins in an infinitesimal interval dx

at point x with negligible relaxation and some scaling e.g. flip angle, main magnetic field strength is

$$s(t) = \int_{object} ds(x,t) = \int_{-\infty}^{\infty} \rho(x) e^{-i\gamma(B_0 + G_x x)t} dx = \left[\int \rho(x) e^{-i\gamma G_x x t} dx \right] e^{-i\omega_0 t} \quad (2.60)$$

In practice, the phase sensitive detection (PSD) or doubly balance mixer or quadrature detector, the method to remove high-frequency from low-frequency band by multiplying signal with reference sinusoidal signal (generated by Frequency synthesizer) and then low-pass-filtering to remove the high-frequency component, has been used [15, 16].

For ambiguity of signal problem, the reference signal which has a 90 degree phase shift relative to the first one has been applied. Figure 2.6 show a diagram of phase sensitive detection.

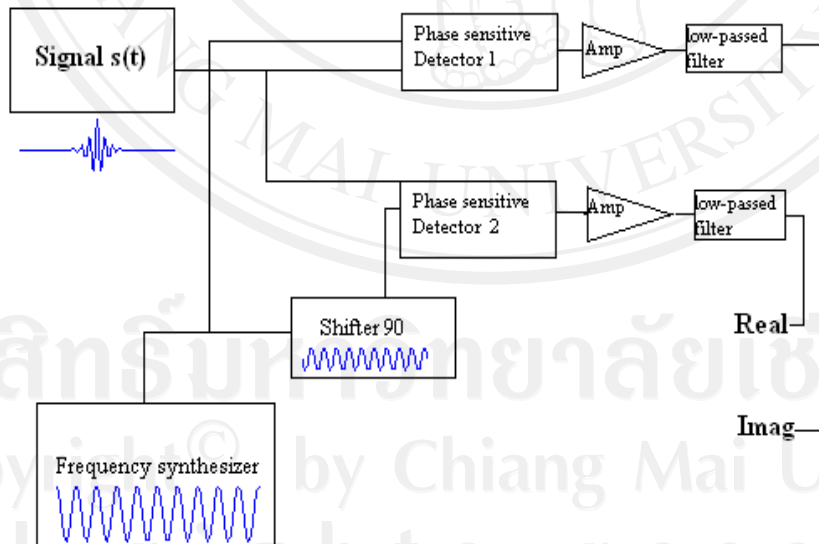


Figure 2.6 shows diagram of PSD that has two detector, amplified low-passed filter, using for remove high frequency component.

Consider the idea of high frequency demodulation, an example of input signal as a sine function oscillating with $(\omega + \Delta\omega)$ is multiplied by 2 reference functions, $\sin(\omega t)$

and $\cos(\omega t)$ and then applies the trigonometric properties, obtaining 2 new functions as in Eq2.61

$$\sin(\omega + \Delta\omega)t \times \sin(\omega t) = \frac{1}{2} \cos(\Delta\omega t) - \cos(2\omega + \Delta\omega)t$$

and
$$\sin(\omega + \Delta\omega)t \times \cos(\omega t) = \frac{1}{2} \sin(\Delta\omega t) + \sin(2\omega + \Delta\omega)t \quad (2.61)$$

The high frequency terms, $\cos(2\omega + \Delta\omega)t$ and $\sin(2\omega + \Delta\omega)t$ from Eq 2.61 are ultimately filtered out by a low-pass filter [16]. After the carrier frequency signal is removed, the general form of FID signal with the gradient received frequency-encoded is

$$s(t) = \int_{object} \rho(r) e^{-i\gamma G_{fe} r t} dr \quad (2.62)$$

where G_{fe} is the frequency-encoding gradient for three planes or $G_{fe} = (G_x, G_y, G_z)$.

Generally, the frequency encoding gradient can be applied only one direction. To perform a multidimensional image, we can either repeat the frequency encoding along other directions or use phase encoding method that will be discussed in next section.

2.3.5 Phase encoding

The phase encoding method encodes the spatial location with different initial phases by applying gradient field in any desired directions. The gradient is turned on only for a short period of time. The signal after the time T_{pe} with signal demodulation will be:

$$s(t) \propto \int_{-\infty}^{\infty} M(r) e^{-i\gamma G_{pe} r T_{pe}} dr \quad (2.63)$$

The phase term is

$$\phi(r) = -\gamma G_{pe} r T_{pe} \quad (2.64)$$

Combining the phase and frequency encoding, we can conveniently encode a 2D or 3D space in any arbitrary coordinates.

2.4 RF PULSE DESIGN

2.4.1 The Small Tip Angle Approximation

2.4.1.1 Fourier relation of RF and M_{xy}

The small-tip angle approximation uses to analyze selective excitation under some conditions. Assuming that the tip angle is small so that $\frac{dM_z}{dt} \approx 0$ and the relaxation T_1 , T_2 will be neglected due to short excitation period compare with the relaxation time. Then the Bloch equation in the rotating frame becomes

$$\begin{pmatrix} \frac{dM'_x}{dt} \\ \frac{dM'_y}{dt} \\ \frac{dM'_z}{dt} \end{pmatrix} = \begin{pmatrix} 0 & \gamma G.r & -\gamma B_{1,y} \\ -\gamma G.r & 0 & \gamma B_{1,x} \\ \gamma B_{1,y} & -\gamma B_{1,x} & 0 \end{pmatrix} \begin{pmatrix} M_x \\ M_y \\ M_z \end{pmatrix} \quad (2.65)$$

Where r is the position vector (x y z) and G = the gradient vector (G_x G_y G_z), the equation 2.65 becomes

$$\begin{aligned} \frac{dM_x}{dt} &= 0 + \gamma G.r M_y - \gamma B_{1,y} M_0 \\ \frac{dM_y}{dt} &= -\gamma G.r M_x + 0 + \gamma B_{1,x} M_0 \\ \frac{dM_z}{dt} &= 0 \end{aligned} \quad (2.66)$$

Define complex notation

$$\begin{aligned} M_{xy} &= M_x + iM_y \\ B_1 &= B_{1,x} + iB_{1,y} \end{aligned} \quad (2.67)$$

Combine the two equations into single equation

$$\begin{aligned} \frac{d(M_x + iM_y)}{dt} &= \gamma G \cdot r M_y - \gamma B_{1,y} M_0 - i(\gamma G \cdot r M_x + \gamma B_{1,x} M_0) \\ d(M_{xy})/dt &= \gamma G \cdot r (-i^2 M_y - iM_x) + \gamma M_0 (i^2 B_{1,y} + B_{1,x}) \\ d(M_{xy})/dt &= \gamma G \cdot r (-i)(M_x + iM_y) + \gamma M_0 (i)(B_{1,x} + iB_{1,y}) \\ d(M_{xy}(r,t))/dt &= -i\gamma G(t) \cdot r M_{xy}(r,t) + i\gamma M_0 B_1 \end{aligned} \quad (2.68)$$

This is 1st order differential equation, and the solution will be

$$M_{xy}(r,t) = iM_0 \int_{-\infty}^T \gamma B_1(t) e^{-i \int_t^T \gamma G(s) \cdot r ds} dt \quad (2.69)$$

Where T is the ending time point of the RF pulse. This equation shows that the transverse magnetization is the Fourier Transform of the applied RF pulse and gradient fields which are in general time-varying.

2.4.1.2 k-space interpretation

k-space is defined as

$$k(t) = -\frac{\gamma}{2\pi} \int_t^T G(s) ds = \frac{\gamma}{2\pi} \int_t^T G(s) ds \quad (2.70)$$

This equation gives the definition of the excitation k-space which is the integral over the remaining gradient. The transverse magnetization of **excitation k-space** will be:

$$M_{xy}(r,t) = iM_0 \int_{-\infty}^T \gamma B_1(t) e^{i2\pi k(t) \cdot r} dt \quad (2.71)$$

We can write the exponential factor as an integral of a three-dimension delta function.

$$\begin{aligned}
 M_{xy}(r, t) &= iM_0 \int_{-\infty}^T \gamma B_1(t) \int_k^3 \delta(k(t) - k) e^{i2\pi k(t).r} dk dt \\
 &= iM_0 \int_k \left[\int_{-\infty}^T \gamma B_1(t)^3 \delta(k(t) - k) dt \right] e^{i2\pi k.r} dk
 \end{aligned}
 \tag{2.72}$$

The bracket is represented by P(k):

$$P(k) = \left[\int_{-\infty}^T \gamma B_1(t)^3 \delta(k(t) - k) dt \right] \tag{2.73}$$

Then P(k) is the Fourier transform (FT) of the magnetization as from Eq.(2.72). If the trajectory in k-space is non singularity, the equation can be rewritten in the form of a unit delta function

$$P(k) = \left[\int_{-\infty}^T \frac{\gamma B_1(t)^3 \delta(k(t) - k) |k'(t)| dt}{|k'(t)|} \right] \tag{2.74}$$

Let W(k) be the spatial weighting function, then

$$W(k) = \frac{\gamma B_1(t)}{|k'(t)|} \tag{2.75}$$

If W(k) is assumed to be a constant,

$$P(k) = W(k) S(k) \tag{2.76}$$

Where

$$S(k) = \int_{-\infty}^T \delta(k(t) - k) |k'(t)| dt$$

Then

$$M_{xy}(r, T) = iM_0 \int_k W(k) S(k) e^{i2\pi k.r} dk \tag{2.77}$$

The transverse magnetization is *the Fourier transform* of a spatial frequency weighting function $W(k)$ multiplied by spatial frequency sampling function $S(k)$. The equation 2.77 implies that we can predict slice profile or behavior of transverse magnetization by Fourier transform of $W(k)S(k)$ and the $W(k)$ can be solved by FT of $w(r)$ or desired shape to be excited.

2.4.2 One-dimensional Selective RF pulse design

2.4.2.1 Simple 1D Selective RF excitation

An example of RF pulse with the nice transform is window-sinc which removes the ripple from truncated Sinc by multiplying Sinc function with a smooth function such as Hanning or Hamming window. Simultaneously with the RF pulse, the slice select gradient, G_z , in trapezoidal shape with a half area refocusing lobe is applied as shown in Figure 2. 7 the Sinc pulses apodized by smooth function windows are described as:

$$B_1(t) = \begin{cases} A \left[(1 - \alpha) + \alpha \cos\left(\frac{2\pi t}{T}\right) \right] \frac{\sin\left(\frac{N2\pi t}{T}\right)}{N2\pi(t/T)} & ; -T/2 \leq t \leq T/2 \\ 0 & \text{Otherwise} \end{cases} \quad (2.78)$$

Where the parameter $\alpha = 0.5$ yields the Hanning window, and $\alpha = 0.46$ for the Hamming window, N is the number of zero crossing point and the amplitude A can be varied to change the tip angle of the pulse. The Hanning window ensures a continuous first derivative where as Hamming window reduces the first derivative at the margins of the symmetric Sinc pulse by factor of 12.5 [16].

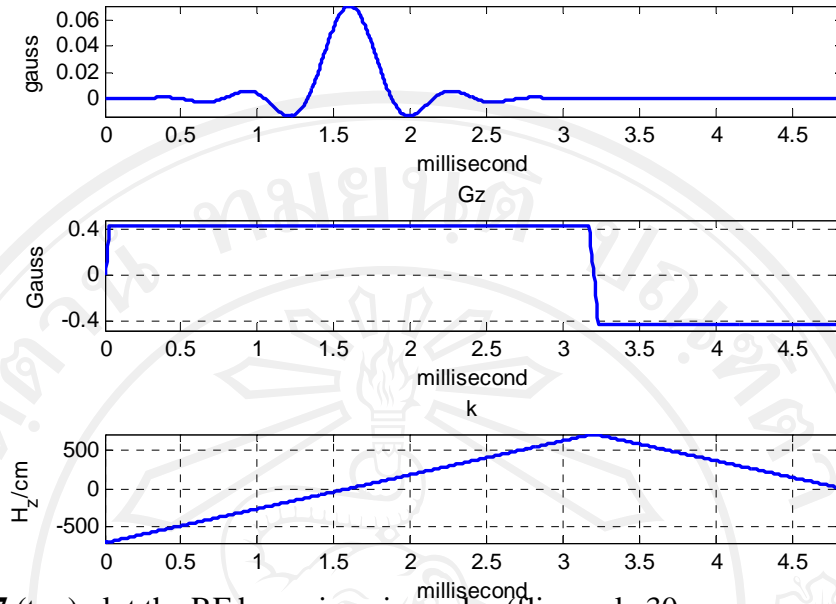


Figure 2.7 (top) plot the RF hamming-sinc pulse (flip angle 30 degree) ,(middle)gradient select slice in z direction and (bottom) show the k-space

From figure 2.7, we used the typical Fourier transform designs of hamming–sinc pulse, calculating the RF amplitude required for any flip angle from the formula:

$$B_{1,max}(t) = \frac{\theta}{\gamma \int_0^t B_1(t) dt} \quad (2.78)$$

For example, the flip angle of 30 degree, we can calculate the bandwidth that is time-bandwidth products of RF pulse which is equal to two times the number of crossing points. Time is the pulse duration or the sampling points multiplied by dwell time, if the pulse duration = 800 sampling points and typical dwell time is 4 microsecond and crossing is 4 points, hence the bandwidth is

$$Bw = (2 \times 4) / 3.2(ms) = 2.5kHz$$

The gradient strength was applied depending on slice thickness and bandwidth by

$$G_{max_required} = \frac{Bw}{\frac{\gamma}{2\pi} (thk)} \quad (2.79)$$

According to the Bloch simulation, the result of the Bloch simulation and the Fourier transform of the RF are represented in figures 2.8;

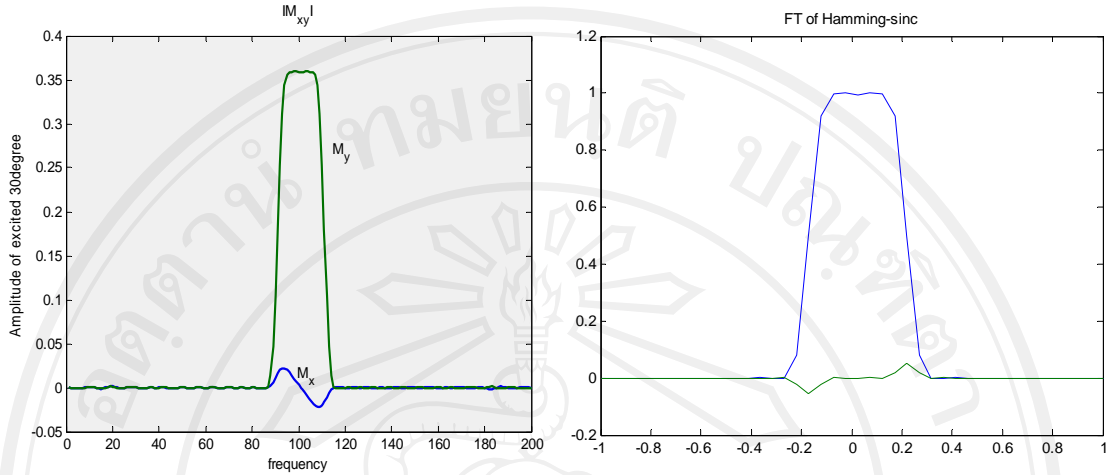


Figure 2.8 Show the result of the Bloch Simulation from an RF excitation of (figure 2.7): (left) 30 degree profile and well refocusing, (right) normalized Fourier Transform of the $B_1(t)$

Note: M_y is imaginary part but the profile of $FT(B_1(t))$ is real part from equations 2.26

2.4.3 Three-Dimensional Tailored RF Pulse Design: Stack spiral

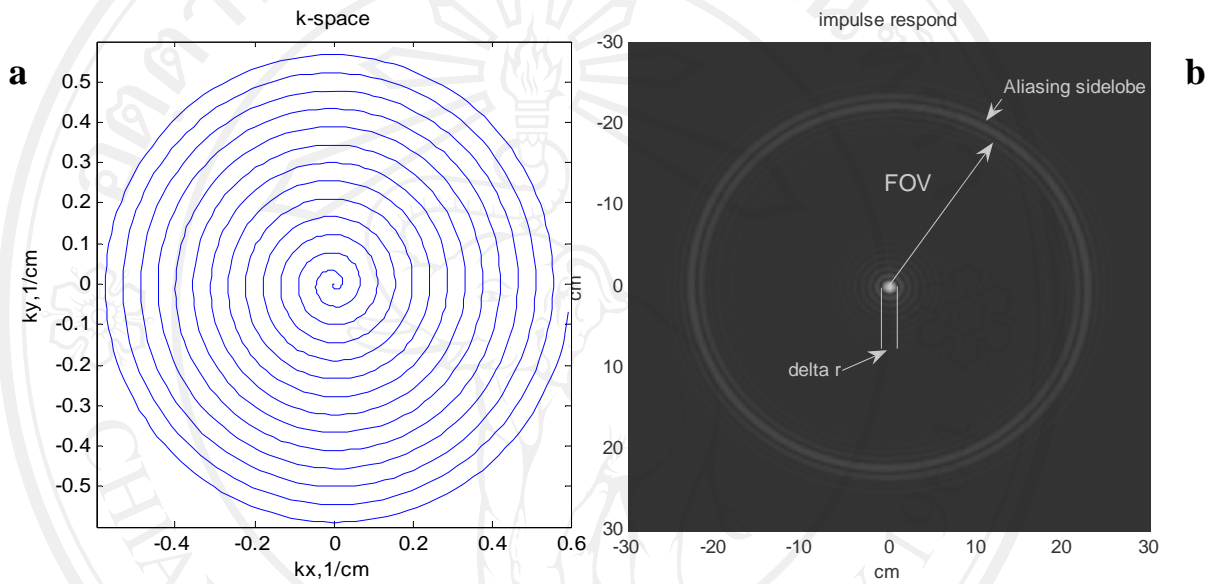
The design of three-dimensional Tailored RF excitation are spatially selective in all three directions at once that affects a volume of magnetization. It has been used in many applications such as correcting for susceptibility artifact and B_1 inhomogeneity [5, 6]. The design base on a 2D spiral trajectory in k_x - k_y plane and gradient blip along k_z such that a cylindrical k-space volume is covered.

The simple 2D spiral trajectories can be generated from the equation below.

$$k(t) = k_{\max} (t/T) e^{i2\pi N(t/T)} \quad (2.80)$$

For spiral outward and constant angular rate, with N = numbers of cycle spiral. T = total pulse width in 2D k space trajectories. The pulse excitation resolution (Δr) and excitation FOV are two important parameters need to be chosen in the trajectory design. Pulse resolution is determined by maximum of k-space and a number of turns

(N) of spiral or how far out of first aliasing side lobe will be is determined by selected excitation FOV as shown in figure 2.9 (a) and (b). The side lobe that from the discreteness and limited extent of the trajectory gives rise to periodic side lobe of excited magnetization (aliasing) and small oscillation (ripples) throughout the periodic interval respectively [13].



Figures 2.9 k-space trajectory design (a) spiral k-space. (b) The impulse respond in image space.

The maximal k-space coverage (k_{\max}), the excitation FOV and N cycles of spiral are determined by[13]:

$$\begin{aligned}
 k_{\max} &= \frac{1}{2\Delta r} \\
 \Delta k &= \frac{1}{FOV} = \frac{2k_{\max}}{2N} \\
 N &= \frac{FOV}{2\Delta r}
 \end{aligned}
 \tag{2.81}$$

Since $k = -\frac{\gamma}{2\pi} G(s) ds$, then

$$dk(t) = \frac{\gamma}{2\pi} G(t) \Delta t
 \tag{2.82}$$

where Δt is the scanner gradient interval typically used 4 microseconds. To avoid aliasing, the maximal $G(t)$ allowed will be:

$$G_{\max} = \max\left(\frac{2\pi}{\gamma\Delta tFOV_{xy}}, g_{\max}\right) \quad (2.83)$$

Where g_{\max} is the scanner maximum gradient limit (typically about 40 mT/m). We always want to obtain a minimal length spiral for given hardware constrains. Thus, accelerate maximal slew rate at the start of spiral until the maximum amplitude is achieved or the k_{\max} is reached. The remaining k-space will be covered by the spiral with constant gradient.

This spiral design algorithm was introduced by Glover (Archimedean spiral)[17]. The weighting function ($W(k)$) for the 2D trajectory can be calculated by the Fourier transform of desired weighting in spatial, e.g. Fermi function ($w(x,y)$) that is

$$W(k) = FT(w(x, y)) \quad (2.84)$$

when

$$w(r) = \frac{1}{1 + e^{(r-r_0)/width}} \quad (2.85)$$

as shown in Figure 2.10

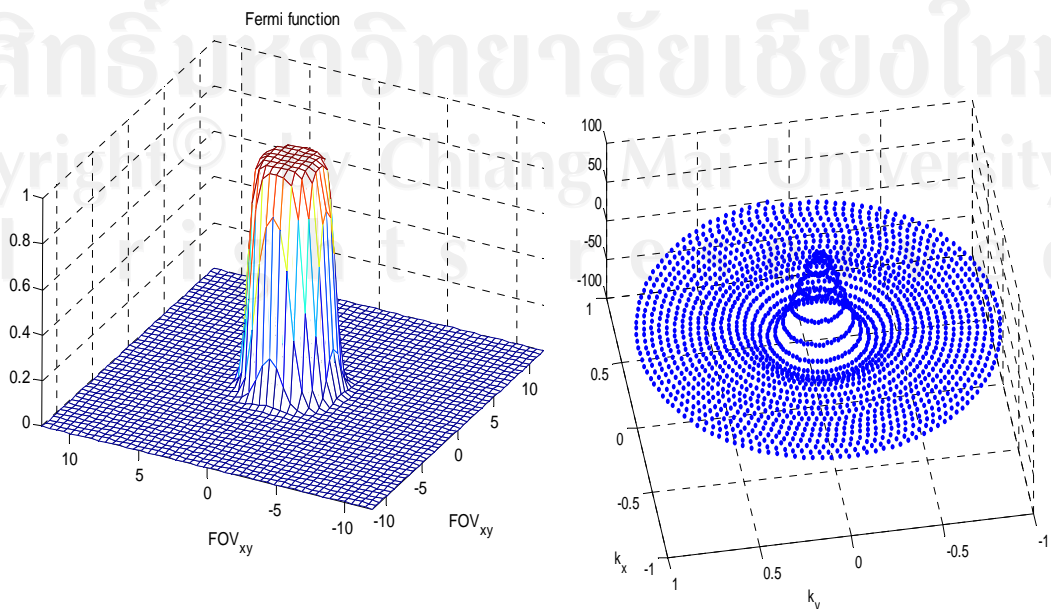


Figure 2.10 Fermi function $w(r)$ (left) and the k-space weighting $W(k(t))$ (right)

From the figure 2.10 we can see Fermi function and the k-space weighting by the Fourier transform of $w(r)$ and weighting to the spiral k-space $W(k(t))$.

To ease the complicated 3D pulse design, a separable design is applied. With **the separable design**, weighting function is composed of through-plane ($P(k_z)$) and in-plane $Q(k_x-k_y)$ as in Eq (2.86)

$$W(k(t)) = Q(k_x, k_y)P(k_z) \quad (2.86)$$

An example of $P(k_z)$ is a Sinc function and the transverse plane is sampled with spiral trajectory obtaining $Q(k_x, k_y)$ which is the in-plane weighting. The through-plane is sampled with blip gradient. The weighting between the through-plane and in-plane is shown in figure 2.11

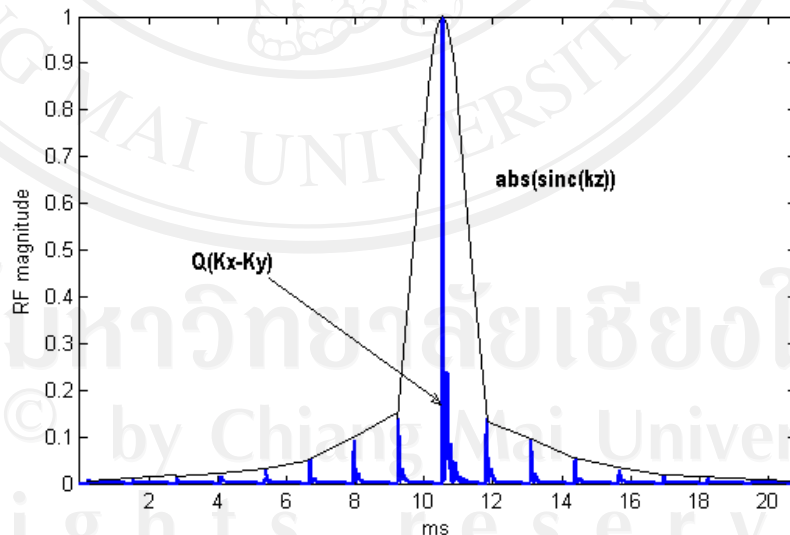


Figure 2.11: 3D TRF pulse design. Diagram of RF magnitude envelope of absolute Sinc in k_z and magnitude in $Q(k_x-k_y)$

Figure 2.11 shows an explanation of this separable design idea. For the stack spirals pulses, $Q(k_x-k_y)$ determines the shape of sub-pulses, and $P(k_z)$ determine the envelope.

The RF waveform $B_1(t)$ is calculated from equation 2.87.

$$B_1(t) = \Delta k(t) | \gamma G(t) | W(k(t)) \quad (2.87)$$

In this thesis, we adopted the 2D spiral trajectories using analytical algorithm developed by Glover[17]. The algorithm was developed from the slew rate limited algorithm of Duyn and Yang[18]. This algorithm includes a modified slew-rate limited case for the trajectory near the origin and switch to amplitude-limited when maximum allowed gradient is being reached. The 2D spiral k-space can also be split into several interleaves for multi-shot excitation to reduce pulse width. The details will be described in chapter 4.

2.4.4 The Half RF pulse (Half-sinc)

In brief, the half-pulse that generally uses for *ultrashort TE imaging* or *short T2 species* has been a topic of recent research [19]. Short T2 components of tissue such as tendons, ligaments, cartilage and bone demonstrate loss of signal from component of tissues or tissues decay rapidly after excitation before the MR system becomes fully operational in receive mode. To minimize T2 decay especially in tissue that has very short T2, splitting RF pulse into two shots call Half-pulse excitation provides shorter feasible TE. To image short T2 species, sequences employing ultrashort echo time (UTE) are required [19]. This section focuses on selective slice excitation using self refocused half-sinc RF pulses. The half-sinc RF excitation pulses are used, limiting the echo time to only the hardware switching time [19]. The half-sinc pulse is *inherently self-refocused* and is applied during the rising and falling slopes of the

slice-selection gradient [20]. The simple RF waveform and the gradients are shown in figures 2.12

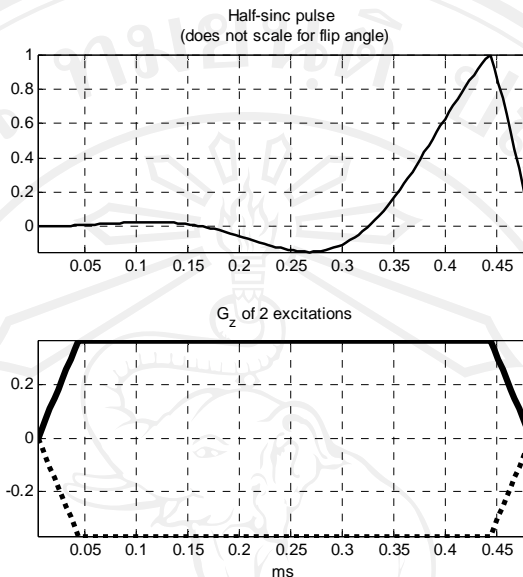


Figure 2.12 (top) The RF wave form which not scale for flip angle (bottom) the slice select gradient wave from of 1st excitation (bold line) and 2nd excitation (dash line).

The half-pulse imaging required fast acquisition such as radial [13] or spiral [19] readout. The idea underlying of half-pulse excitation was first proposed by JM Pauly [21] for the imaging of very short T₂ species. A simple conventional excitation, which shows in figure 2.7, consists of a slice selective RF excitation followed by gradient refocusing interval. The k-space is traversed from k-space minimum (k-min) to k-space maximum (k-max) and then returns to origin or zero of k-space. In contrast, the proposed half-pulse excitation method eliminates the post-excitation refocusing. The half-pulse selective excitation diagram is illustrated in figure 2.12 which consists of 2 excitations. The first half-excitation played out in the presence of a positive gradient, beginning at the k-min an end at k-space origin (self refocusing). For the second half-excitation, the opposite gradient was applied, which implies a linearity of k-trajectory

beginning at k-max and again ending at the origin. Once both pulses have been applied, the traversal through excitation k-space is completed as shown in figure 2.13

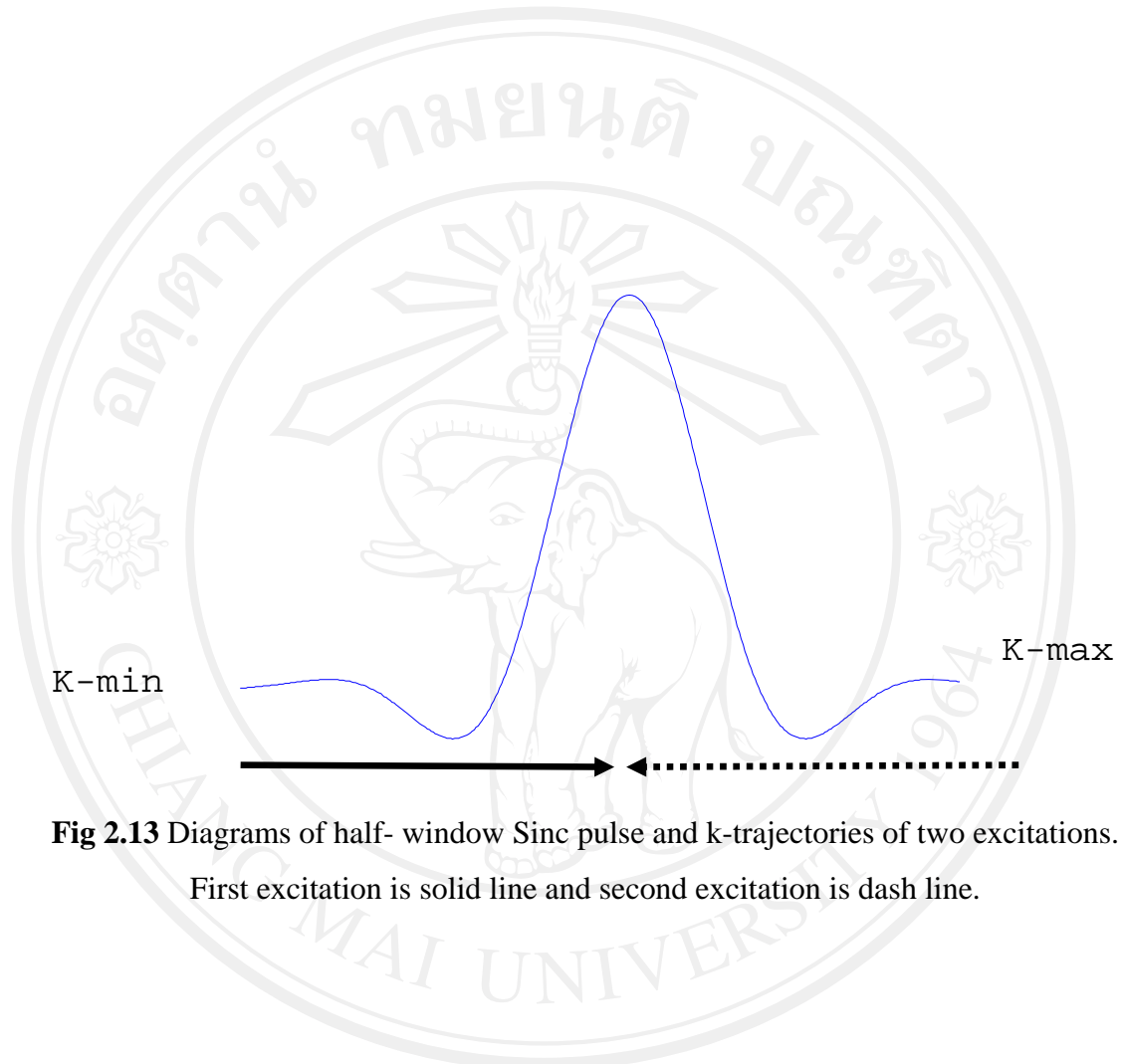


Fig 2.13 Diagrams of half- window Sinc pulse and k-trajectories of two excitations.
First excitation is solid line and second excitation is dash line.